Available online at www.sciencedirect.com
SCIENCE DIRECT®
Journal of Organometallic Chemistry 690 (2005) 383–393
Journal of Organometallic Chemistry
www.elsevier.com/locate/jorganchem

Synthesis and structural characterization of *N*-*para*-ferrocenyl benzoyl amino acid ethyl esters and the X-ray crystal structures of the glycyl and (±)-2-aminobutyric acid derivative $Fc\text{-}C_6H_4CONHCH(C_2H_5)CO_2Et$

David Savage [a], Gwen Malone [a], John F. Gallagher [a,b,*], Yoshiteru Ida [c], Peter T.M. Kenny [a,b,*]

[a] *School of Chemical Sciences, Dublin City University, Dublin 9, Ireland*
[b] *National Institute of Cellular Biotechnology, Dublin City University, Dublin 9, Ireland*
[c] *School of Pharmaceutical Sciences, Showa University, Hatanodai, Shinagawa-ku, Tokyo 142-8555, Japan*

Received 1 August 2004; accepted 1 August 2004
Available online 22 October 2004

Abstract

A series of *N*-*para*-ferrocenyl benzoyl amino acid ethyl esters **1–8** have been prepared by coupling *para*-ferrocenyl benzoic acid with the amino acid esters using the conventional 1,3-dicyclohexylcarbodiimide (DCC), 1-hydroxybenzotriazole (HOBt) protocol. The amino acids employed in the synthesis were glycine, L-alanine, L-leucine, L-phenylalanine, β-alanine, 4-aminobutyric acid, (±)-2-aminobutyric acid and 2-aminoisobutyric acid. The compounds were fully characterized by a range of spectroscopic techniques such as NMR and mass spectrometry. In addition the X-ray crystal structures of the glycyl **1** and (±)-2-aminobutyrate **7** derivatives have been determined. Analysis of relevant fragments in crystal structures on the Cambridge Structural Database indicates a relative paucity of common fragments such as the α-aminobutyrate group in comparison to the glycyl moiety.

Keywords: Ferrocene; Bioorganometallic chemistry; Amino acid esters; X-ray crystal structures; Database analysis; Systematics

1. Introduction

The organometallic compound ferrocene is a promising candidate for incorporation in novel materials due to its stability, spectroscopic, electrochemical properties and ease of use [1]. As a direct consequence of these properties, research in the area of ferrocenyl derivatives has seen a dramatic increase in attention over the past decade, primarily for the ultimate goals of achieving novel sensor compounds, peptide mimetic models and unnatural drugs [2–10]. The synthesis and structural characterization of a variety of *N*-ferrocenoyl and *N*-ferrocenyl amino acid and peptide derivatives has been reported [11–25]. We now report the synthesis of a series of *para*-ferrocenyl benzoyl amino acid ethyl esters **1–8**. The ferrocenyl moiety is linked to the amino acid residues through a *para*-benzoyl group. The compounds were fully characterized by ^1H NMR, ^{13}C NMR spectroscopy and mass spectrometry. In addition the X-ray crystal structures of compounds **1** and **7** are reported and compared with a related structure [22]. The compounds are composed of three key moieties, namely (i) an electroactive core, (ii) a conjugated linker that can act as a chromophore and (iii) an amino acid derivative that can interact with other molecules via hydrogen bonding.

* Corresponding authors. Tel.: +353 1 7005689; fax: +353 1 7005503.
E-mail addresses: john.gallagher@dcu.ie (J.F. Gallagher), peter.kenny@dcu.ie (P.T.M. Kenny).

0022-328X/$ - see front matter © 2004 Elsevier B.V. All rights reserved.
doi:10.1016/j.jorganchem.2004.08.047

2. Results and discussion

2.1. Synthesis

para-Ferrocenyl benzoic acid was prepared as previously reported [22]. This acid was coupled under basic conditions to the free *N*-terminal amino acid esters of glycine, L-alanine, L-leucine, L-phenylalanine, β-alanine, 4-aminobutyric acid, (±)-2-aminobutyric acid and 2-aminoisobutyric acid in the presence of dicyclohexylcarbodiimide (DCC) and 1-hydroxybenzotriazole (HOBt). The resulting *N*-*para*-ferrocenyl benzoyl amino acid esters **1–8** were obtained as yellow/orange colored crystals (Scheme 1). The yields obtained ranged between 48% and 68% and all gave analytical and spectroscopic data in accordance with the proposed structures. The compounds are reasonably stable however they slowly decompose over a period of time. The *N*-*para*-ferrocenyl benzoyl ethyl esters **1–8** were characterized by a combination of ^{1}H NMR, ^{13}C NMR, DEPT-135 and ^{1}H–^{13}C COSY (HMQC) spectroscopy and by either fast atom bombardment (FAB) **1–4**, electrospray ionization (ESI) **5**, **6** or matrix assisted laser desorption ionization mass spectrometry (MALDI) **7**, **8**. Crystals of sufficient quality for X-ray diffraction studies were obtained for compounds **1** and **7**.

2.2. ^{1}H and ^{13}C NMR spectroscopic analysis

All the proton and carbon chemical shifts for compounds **1–8** were unambiguously assigned by a combination of DEPT-135 and ^{1}H–^{13}C-COSY (HMQC). The ^{1}H and ^{13}C NMR spectra for compounds **1–8** showed peaks in the ferrocene region characteristic of a mono substituted ferrocene moiety [4,5,22]. The protons in the *ortho* position of the substituted Cp ring appear in the region δ 4.65–4.89 whereas the protons in the *meta* position occur in the range δ 4.17–4.41. The unsubstituted Cp ring appears in the region δ 3.77–4.02. The protons of the *para*-disubstituted benzoyl group appear as two doublets in the region δ 7.38–7.8. For example, in the case of the β-alanine derivative **5**, the aromatic protons are present as two doublets at δ 7.61 and δ 7.76, respectively. The unsubstituted C_5H_5 ring appears as a singlet in the ^{1}H NMR spectrum at δ 4.01 whereas the *ortho* and *meta* protons on the substituted Cp ring are present at δ 4.87 and δ 4.39, respectively. The N*H* proton appears as a triplet at δ 8.56 (J = 5.2 Hz) and a quartet at δ 3.5 (J = 7.2 Hz) corresponds to the NHC$\underline{H_2}$CH$_2$CO-protons. The triplet at δ 2.59 (J = 7.2 Hz) is due to the second methylene group adjacent to the carbonyl group.

The ^{13}C NMR spectra of compounds **1–8** show signals in the region δ 66.9–83.9 indicative of a monosubstituted ferrocene subunit [4,5,22]. The *ipso* carbon of the substituted Cp ring appears in a narrow range of δ 83.5–83.9. This signal is not present in the DEPT 135 spectra. The carbon atoms of the aromatic ring are visible in the region δ 125.7–144.2. The methylene carbon atoms of the derivatives were identified by DEPT-135. A complete assignment of the ^{1}H and ^{13}C NMR spectra of *N*-{*para*-(ferrocenyl)benzoyl}-β-alanine ethyl ester **5** is presented in Table 1.

2.3. Mass spectrometry

Since the introduction of soft ionization techniques such as fast atom bombardment mass spectrometry (FABMS), electrospray ionization mass spectrometry (ESIMS) and matrix assisted laser desorption ionization (MADLI), a wide range of thermolabile and non-volatile compounds can be subjected to mass spectrometric analysis [26–29]. As the compounds were not amenable to electron ionization studies, the soft ionization techniques were employed in the analysis and confirmed the correct relative molecular mass. Examination of the mass spectra revealed the presence of both radical-cation $[M]^{+\bullet}$, and protonated molecular ion species, $[M + H]^{+}$. The abundance of the

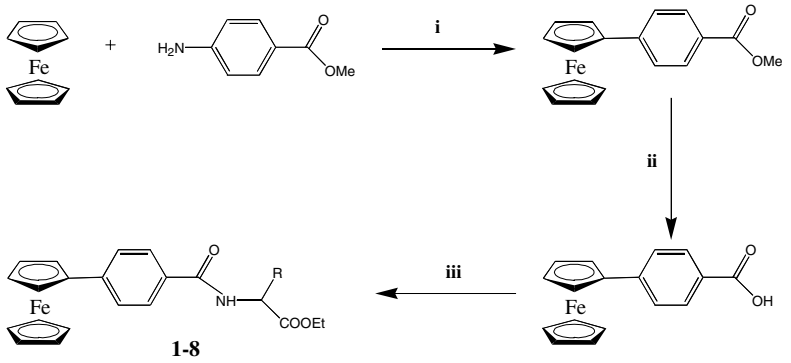

Scheme 1. Synthesis of the *N*-ferrocenylbenzoyl amino acid esters **1–8**, (i) $NaNO_2$, HCl, 5 °C, (ii) NaOH/MeOH, (iii) DCC, HOBt, Et_3N, Amino acid ethyl ester.

Table 1
^{1}H and ^{13}C spectroscopic data for **5**

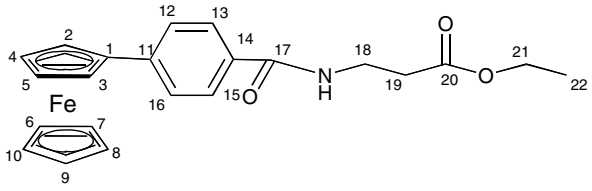

Site	^{1}H NMR	^{13}C NMR	HMQC
1		83.6	
2,3	4.87		66.9
4,5	4.39		69.8
6–10	4.01		69.8
11		143	
12, 16	7.61		125.7
13, 15	7.76		127.7
14		131.7	
17		166.5	
18	3.5		34.2
19	2.59		31
20		171.7	
21	4.07		60.3
22	1.18		14

Table 2
Selected bond lengths and angles (Å, °) for molecules A/B in **1**, and **7**

	A/B in **1**	**7**
Fe1…Cg1	1.635(3)/1.643(3)	1.6472(13)
Fe2…Cg2	1.648(4)/1.645(4)	1.6485(16)
Cg1…Fe1…Cg2	177.7(2)/179.41(15)	179.50(16)
C1–O1	1.248(7)/1.243(7)	1.232(3)
C3–O2	1.203(7)/1.193(7)	1.180(3)
C3–O3	1.317(7)/1.345(7)	1.332(3)
C1–N1	1.327(8)/1.324(8)	1.330(3)
C2–N1	1.439(7)/1.440(7)	1.462(3)
C2–C3	1.499(8)/1.499(8)	1.526(4)
C1–C34	1.490(8)/1.498(8)	1.506(3)
Fe1–C11–C31	125.5(4)/126.9(4)	128.54(18)
O1–C1–N1	121.3(6)122.1(6)	123.0(3)
O1–C1–C34	121.5(6)/121.6(6)	121.5(2)
C1–N1–C2	124.2(6)/124.7(6)	122.2(2)
N1–C1–C34	117.1(6)/116.4(6)	115.5(2)
N1–C2–C3	112.0(5)/111.5(5)	107.5(2)
N1–C2–C6	–/–	113.3(2)
Fe1–C11–C31–C36	65.0(8)/110.4(6)	118.9(2)
C12–C11–C31–C36	−23.3(10)/19.2(10)	27.6(4)
N1–C1–C34–C33	−157.0(6)/153.1(6)	143.3(3)
C2–N1–C1–C34	176.3(6)/175.5(5)	−179.0(2)
C1–N1–C2–C3	−107.5(7)/120.3(7)	126.9(3)
N1–C2–C3–O3	−160.8(6)/156.1(6)	150.9(2)

where Cg1/Cg3 and Cg2/Cg4 are the centroids of the (η^5-C_5H_4)/(η^5-C_5H_5) rings in molecules A and B in **1**, respectively.

$[M + H]^+$ species was greatest in the analysis of samples **5** and **6** by ESI. However analysis of compounds **1–4** by FAB and **7** and **8** by MALDI generated radical-cations $[M]^{+\cdot}$ as the most abundant species. Cation adducts corresponding to $[M + Na]^+$ and $[M + K]^+$ were also present. Addition of a dilute solution of potassium iodide (KI) to samples **1–4** and the liquid matrix on the probe tip generated an intense signal 39 Daltons higher due to an $[M + K]^+$ adduct. The vast majority of analytes subjected to analysis by FAB and MALDI furnish protonated molecular ion species or cation adducts [26,28,29]. It has been reported that the molecular radical cation of ferrocene and not the protonated molecule is generated during analysis by MALDI [30]. Structurally significant fragment ions were observed in the FAB mass spectra for compounds **1–4**. A fragment ion is present at *m/z* 261 confirming the presence of a ferrocenylphenyl subunit at the *N*-terminal. The signal present at *m/z* 289 is due to cleavage at the benzoyl C═O function. This fragment ion at *m/z* 289 was also observed in the MALDI and ESI spectra.

2.4. X-ray crystallographic studies of *1* and *7*

The single crystal X-ray structures of **1** and **7** have been determined, with selected bond lengths and angles listed in Table 2 with crystallographic details given in the *footnote*. The molecular and crystal structures of both **1** and **7** are also compared with the previously reported *N*-{para-(ferrocenyl)benzoyl}-L-alanine methyl ester **9** [22]. There is an increasing number of metallocene based amino acid/peptide structures on the Cambridge Structural Database (CSD) [31], however research on compounds incorporating the Fc–C_6H_4- moiety are still relatively rare in comparison to the plethora of Fc systems reported, where Fc = (η^5-C_5H_5)Fe(η^5-C_5H_4).

2.4.1. Molecular and crystal structure study of *1*

The glycine derivative **1** (Fig. 1) contains two molecules, which differ significantly in conformation in the asymmetric unit of space group $P2_1/c$ (No. 14). The ferrocenyl (η^5-C_5) cyclopentadienyl groups are slightly staggered with C1*n*…Cg1…Cg2…C2*n* torsion angles (*n* = 1–5) in the range 9.5(8)–11.5(7)° and 7.9(6)–8.9(5)° for molecules A and B, respectively. The Fe1A…Cg1/Cg2 distances are 1.635(3)/1.648(4) Å, while the Cg1…Fe1…Cg2 angle is 177.7(2)°: corresponding data for Fe1B…Cg3/Cg4 in B are 1.643(3)/1.645(4) Å and 179.41(15)° (where Cg1/Cg3 and Cg2/Cg4 are the centroids of the (η^5-C_5H_4) and (η^5-C_5H_5) rings in A/B, respectively). The most important geometric parameters are amide C═O 1.248(7)/1.243(7) Å, OC–NH 1.327(8)/1.324(8) Å, HN–CH 1.439(7)/1.440(7) Å, ester C═O/CO 1.203(7)/1.317(7) Å and 1.193(7)/1.345(7) Å, respectively, which are similar to the dimensions in previously reported systems, such as the L-alanine derivative **9** [22]. Other important bond length/angle parameters are listed for comparison in Table 2 and will be discussed for both systems 1 and 2.

The most important structural feature in **1** is the orientation of the carboxylate group with respect to the

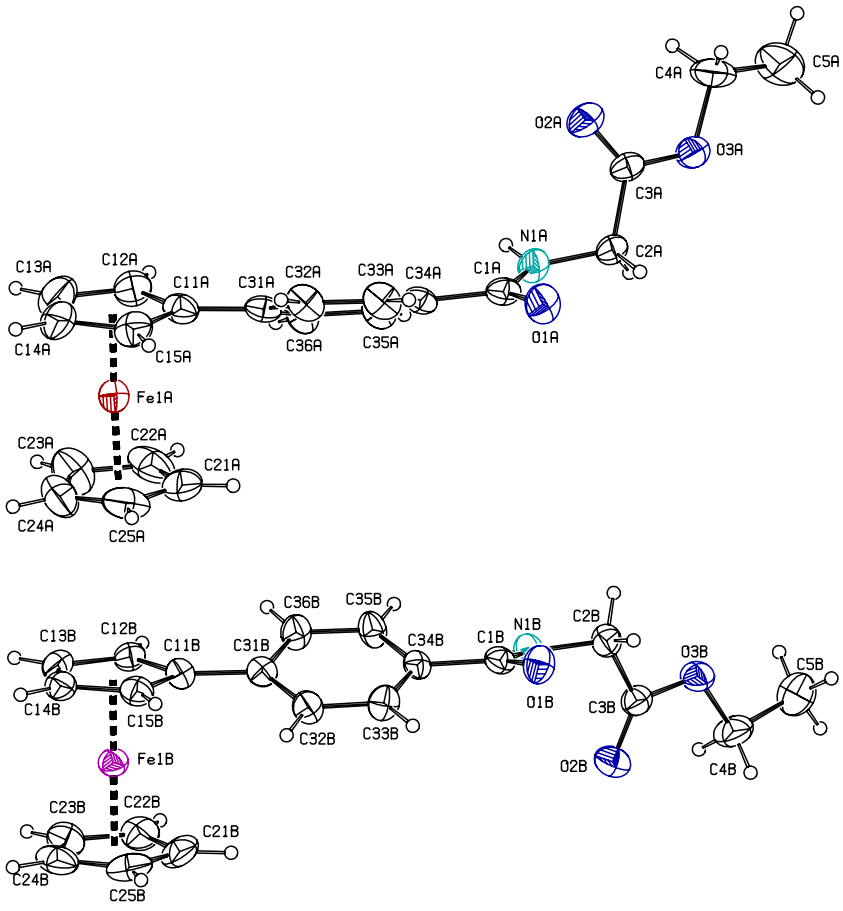

Fig. 1. Molecular diagrams of the independent molecules A/B in **1**: displacement ellipsoids are drawn at the 30% probability level.

ferrocenyl moiety in molecules A and B. Key differences are evident both from an examination of the ORTEP diagrams and the torsion angles listed in Table 2. Molecule A has the carboxylate group oriented in a *transoid* fashion relative to the unsubstituted (η^5-C_5H_5) ring (and similar to the conformation of the L-alanine derivative **9**), whereas molecule B has the carboxylate group oriented in a *cisoid* conformation and similar to that observed in **7** detailed below. For example, the torsion angles for C1–N1–C2–C3 are −107.5(7)/120.3(7)° in **1** and 126.9(3)° in **7**, in comparison to −67.4(2)° in the L-alanine derivative **9**. These differences highlight the flexibility of these Fc–C_6H_4–CONH–X systems in adopting quite different conformations through rotation of groups about the N1–C2 bond.

The plane data also highlight considerable differences between molecules A and B. The angle between the –C_6H_4– ring and the fouratom plane O=C–N–C is 23.7(4)/28.4(4)° and between the –C_6H_4–/(η^5-C_5H_4) rings, 23.2(2)/18.9(4)°: whilst the angle between the substituted (η^5-C_5H_4) ring and the O=C–N–C plane is 8.4(5)/10.5(5)°. Although the plane data look similar, the central C_6 aromatic ring is twisted in opposite directions in A and B, respectively, with respect to the η^5-C_5H_4 and O1/C1/N1/C2 groups flanking on either side (these are almost mutually co-planar). The carboxylate groups are almost orthogonal to the four atom amide residues at 81.0(3)/73.8(3)°. Nonetheless, it is the torsion angle data that provides the relative orientation of the carboxylate groups with respect to the ferrocenyl groups (Figs. 1 and 2).

The primary intermolecular interactions in **1** (Table 3) are two separate NH...O=$C_{(amide)}$ hydrogen bonds which generate two independent (A...A..)$_n$ and (B...B..)$_n$ one-dimensional chains along the *b*-axis with graph set C(4). These are typical amide...amide intermolecular interactions (Fig. 2). The $N1_{(A/B)}\cdots O1^{b}_{(A/B)}$ distances are 2.801(7) and 2.994(8) Å, respectively, with $N1_{(A/B)} - H1_{(A/B)}\cdots O1^{b}_{(A/B)}$ angles of 172(7)° and 167(5)°. The packing along each of the chains comprises alternating 'head to tail' arrangements of identical molecules along the 2_1 axis as two independent A or B chains and (repeated at every unit cell), with symmetry codes (for A^b, $-x$, $-1/2 + y$, $1/2 - z$ or 2_545) and (for B^b, $1 - x$, $1/2 + y$, $1/2 - z$ or 2_655) as used in Fig. 2. These independent chains are linked together through two

Table 3
Intermolecular Interactions (Å, °) for molecules A/B in **1**, and **7**

1					
DH...A[a]	D–H	H...A	D...A	D–H...A	Symmetry[b]
N1A–H1A...O1A	0.91(8)	1.89(8)	2.801(7)	172(7)	2_545
N1B–H1B...O1B	0.92(6)	2.09(6)	2.994(8)	167(5)	2_655
C4B–H4B2...O1A	0.97	2.56	3.310(8)	134	1_655
C36B–H36B...O2A	0.93	2.50	3.390(8)	161	2
C2A–H2A2...O1A	0.97	2.41	2.786(8)	103	Intra
C2B–H2B1...O1B	0.97	2.42	2.808(8)	104	Intra
7					
N1–H1...O1	0.80(3)	2.18(3)	2.962(3)	165(2)	2_655
C2–H2...O1	0.98	2.35	2.787(3)	106	Intra
C4–H4B...O1	0.97	2.52	3.353(4)	145	3_666
C36–H36...O2	0.93	2.52	3.391(3)	157	4_575

[a] D–H...A signifies Donor–Hydrogen...Acceptor.
[b] Symmetry operations as detailed in the text and from SHELXL97. In Figs. 2 and 4, suffixes are used for simplicity to designate the symmetry related molecules.

weaker C–H...O interactions into 2D sheets through C4B...O1A^{i} 3.310(8) Å and C36B...O2A^{ii} 3.390(8) Å interactions (with symmetry operations: (i) $1 + x$, y, z and (ii) $-x$, $-1/2 + y$, $1/2 - z$). In Fig. 2 the # and $ represent the $R_3^3(21)$ and $R_5^4(23)$ rings, thus generated by the C–H...O interactions. Aggregation of the two independent chains occurs in solution through N–H...O=C$_{(amide)}$ interactions and upon crystallization the packing in the crystal structure retains two distinct t*ransoid* and *cisoid* type conformations linked through N–H...O=C hydrogen bonds (Fig. 2). This is not unusual and structures with more than one molecule in the asymmetric unit are a common though largely unexplained occurrence. There is no significant C–H...π(arene) or π...π stacking interactions in **1**.

2.4.2. Molecular and crystal structure study of 7

In the (±)-butyrate derivative **7**, one molecule is present in the asymmetric unit in space group $P2_1/c$ (Fig. 3). The ferrocenyl (η^5-C_5) groups are essentially eclipsed with torsion angles C1*n*...Cg1...Cg2...C2*n* (n = 1–5) in the range 4.0(3)–4.6(2)°. The Fe1...Cg1/Cg2 distances are 1.6472(13)/1.6485(16) Å, while the Cg1...Fe1...Cg2 angle is almost linear at 179.50(8)° (where Cg1 and Cg2 are the centroids of the (η^5-C_5H_4) and (η^5-C_5H_5) rings, respectively). Important geometric parameters include amide C=O 1.232(3) Å, OC–NH 1.330(3) Å, HN–CH 1.462(3) Å and ester C=O/C–O 1.180(3)/1.332(3) Å, respectively, and similar to the dimensions in **1**. Major differences to note are N1–C2–C3, 112.0(5)/111.5(5)° in **1**, 110.24(16)° in **9**, 107.5(2)° in **7** giving a spread of 5° at C2. On substituting H by CH_3 and CH_2CH_3 along the three compound structural series, the increasing steric congestion is reflected in a contraction of this angle at C2 in **7**.

The primary intermolecular interaction in **7** (Table 3) is N–H...O=C(amide) generating a one-dimensional chain along the *b*-axis with graph set C(4), N...O^{b} 2.962(3) Å, NH...O^{b} 165(2)° (symmetry code, (b) $1 - x$, $1/2 + y$, $1/2 - z$ or 2_655). This interaction is ca. 0.15 Å longer than the N–H...O=C$_{(amide)}$ hydrogen bond in the (A...A..)$_n$ chain of 1 though slightly shorter by 0.03 Å than in the (B...B..)$_n$ chain. There are two CH...O intermolecular interactions present in **7**, which are longer, with C...O distances of 3.353(4), 3.391(3) Å, the former along the *a*-axis direction (Fig. 4). There are no significant C–H...π(arene) or π...π stacking interactions.

In **7** the –C_6H_4– ring and the fouratom O=C–N–C plane are oriented at 36.94(16)° and for the –C_6H_4–/(η^5-C_5H_4) rings, 27.91(18)°: whereas the angle between (η^5-C_5H_4) and the O=C–N–C plane is 9.1(3)°. As viewed in Fig. 3, these data show a significant twist between the central C_6 aromatic ring and the two moieties flanking on either side (which are almost mutually coplanar). These results serve to demonstrate the flexibility in the orientation of these rings/planes in the molecular structures of **1**, **7** and **9** in the solid state. The carboxylate and ethyl groups at C2 in **7** are distinctly different from **1** though more similar to molecule B in **1**. In **7** the angles C1–N1–C2–C3/N1–C2–C3–O2, 126.9(3)°/−33.0(4)° also contrast with −67.4(2)°/−26.5(2)° in **9**. From above, structure **7** retains a *cisoid*-type conformation in contrast to the *transoid* conformation in **9** and in A (**1**).

2.4.3. Analysis of fragments in the cambridge structural database

A search of the Cambridge Structural Database (January 2004 – version v5.25) for structures incorporating the C–N(H)–C(Et)(H)CO_2 moiety (for *N*-substituted systems) reveals that it is a system which had been barely studied when compared to the more common amino acid derivatives, e.g. glycine or L-alanine

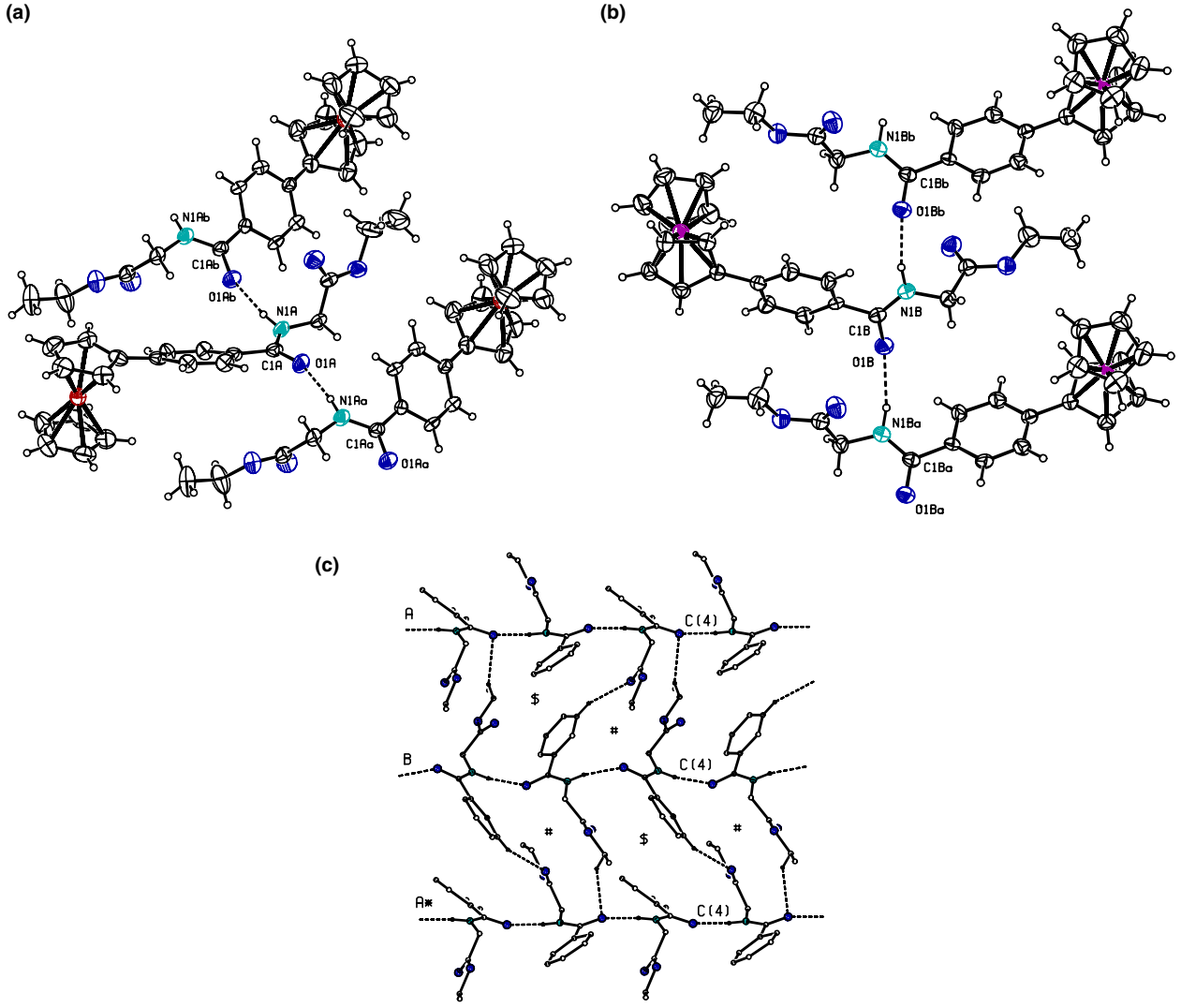

Fig. 2. Three packing diagrams of **1** (a) and (b) as ORTEP diagrams of the A and B chains (suffixes for symmetry related molecules) and (c) as a PLATON diagram with A, B and A* chains (along the *b*-axis) linked by the C–H. . .O hydrogen bonds (along the *a*-axis). The # and $ represent the hydrogen bonded $R_3^3(21)$ and $R_5^4(23)$ rings, respectively. Atoms not involved in interactions have been removed for clarity apart from the molecular backbone.

(CSD searches were undertaken with no restrictions as depicted in Scheme 2) [31]. Three important structures that have been reported are ACDAHO, α-(acetyl)-D-amino-butyric acid monohydrate [32]; KIHZAC, N-(3-indolylacetyl)-α-amino-L-butyric acid [33] and XOSHUI, 2-(L-alanylamino)-L-butyric acid hydrate [34], results obtained from seven 'hits' incorporating the 'C–N(H)–C(Et)(H)CO_2' fragment (Scheme 2). However, all three of these derivatives crystallized from a chiral form and in the acentric space groups, e.g. $P2_12_12_1$ and $P2_1$, unlike **7** which crystallized from a racemic material into the centric space group $P2_1/c$ (No. 14).

The parent amino acid DL-α-amino-*n*-butyric acid has been the subject of crystal structure analyses by several research groups (at different temperatures) over several decades, the most precise of which has been reported with CSD code, DLABUT05 [35]. The search for 'N(H)-C(Et)(H)CO_2' fragments yielded 27 'hits', most of which are zwitterions with the N atom protonated as NH_3^+, carboxylate as CO_2^- or as metal complexes, e.g. Cu bonded in a bidentate fashion to the amino N and carboxylate O atoms.

A more common fragment is that of 'C–N(H)–C(Et)CO_2' which is present in diethylglycine, isovaline and *n*-butylethylglycine derivatives amongst others. Even for this fragment there are only 42 'hits' when compared to the *N*-substituted glycine fragment 'C–N(H)–CH_2CO_2' which yields a total of 1276 'hits' (Scheme 2) on the CSD. Interestingly, in terms of the current study there are 32 structures on the CSD which contain a (η^5-C_5)Fe(η^5-C_5) moiety in combination with a HN–C–CO_2 fragment and representative of the ferrocenyl amino acid and peptides on the CSD and research activity in the area to date.

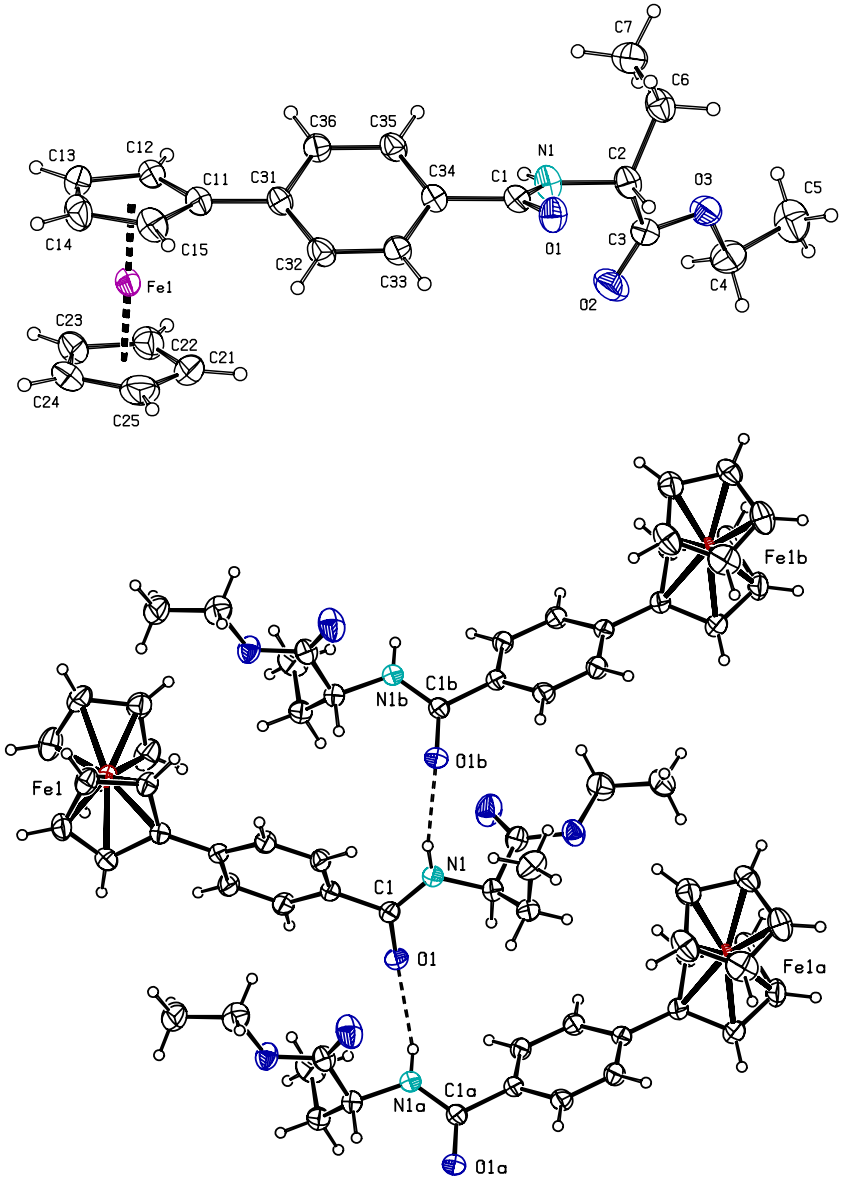

Fig. 3. Molecular diagram of **7** (top) and a packing diagram (bottom) showing the N–H. . .O=C hydrogen bonded chain using ORTEP (suffixes for symmetry related molecules): displacement ellipsoids are drawn at the 30% probability level.

3. Summary

The *N-para*-ferrocenyl benzoyl amino acid ethyl esters **1–8** have been prepared by coupling *para*-ferrocenyl benzoic acid with the amino acid esters using the conventional 1,3-dicyclohexylcarbodiimide (DCC), 1-hydroxy- benzotriazole (HOBt) protocol The compounds were fully characterized by a range of spectroscopic techniques such as NMR and mass spectrometry.

The X-ray crystal structures of the glycyl **1** and (±)-2-aminobutyrate **7** derivatives have been determined. Analysis of relevant fragments in crystal structures on the Cambridge Structural Database indicates a relative paucity of common fragments such as the α-aminobutyrate group in comparison to the glycyl moiety.

4. Experimental

4.1. General procedures

All chemicals were purchased from Sigma/Aldrich and used as received. Commercial grade reagents were used without further purification, however, solvents were purified prior to use. Melting points were determined using a Griffin melting point apparatus and are uncorrected. Infrared spectra were recorded on a Nicolet 405 FTIR spectrometer and UV–Vis spectra on a Hewlett–Packard

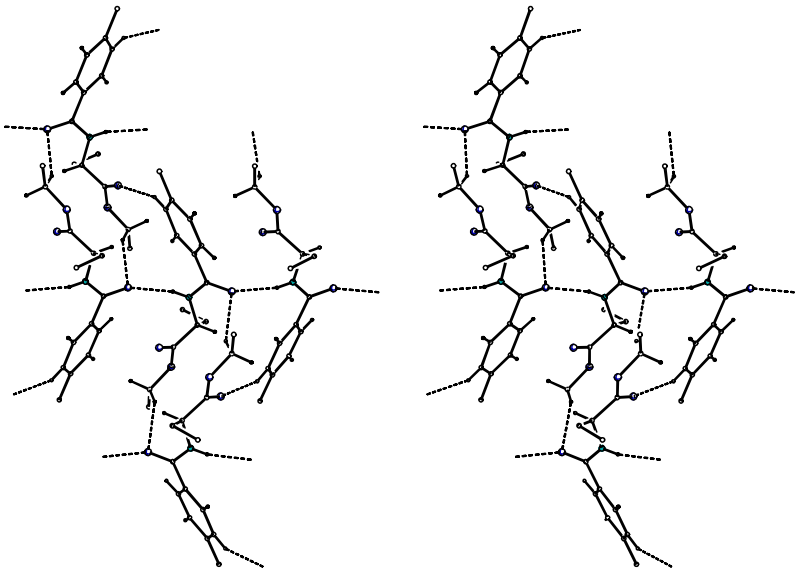

Fig. 4. A stereoview of the important intermolecular interactions in **7**. The ferrocenyl moiety and ethyl H atoms have been removed for clarity. The hydrogen bonding rings can be clearly discerned and comprise the C(4) chain and hydrogen bonded ring motifs.

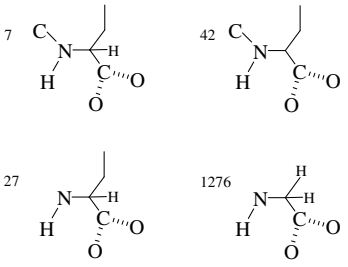

Fragments used and 'hits' found in the CSD searches

Scheme 2. Cambridge Structural Database fragment search.

8452A diode array UV–Vis spectrophotometer. NMR spectra were obtained on a Bruker AC 400 NMR spectrometer operating at 400 MHz for ^{1}H NMR and 100 MHz for ^{13}C NMR. The ^{1}H and ^{13}C NMR chemical shifts (ppm) are relative to TMS and all coupling constants (*J*) are in Hertz. Positive ion fast atom bombardment mass spectra were obtained on a JEOL SX102 double focussing mass spectrometer employing *meta*-nitrobenzyl alcohol as the liquid matrix. Electrospray ionization mass spectra were obtained on an Applied Biosystems QSTAR quadrupole time of flight mass spectrometer and matrix assisted laser desorption ionization mass spectra on a Bruker Ultraflex TOF/TOF mass spectrometer employing a nitrogen laser at 337 nm.

The single crystal X-ray data for **1** and **7** were collected on a Siemens P4 diffractometer at 294(1) K: ω-scans for the θ range 2–26°. Data reductions for both compounds were standard with the absorption correction DIFABS used for **1** and ψ-scans were used for the absorption correction to **7** (6 reflections with 4° increments). The structures were solved by direct methods and refined using full matrix least squares methods using SHELXS97 and SHELXL97, respectively [36]. Hydrogen atoms were treated as riding atoms except for the amino H atom, which was refined with isotropic displacement parameters in both structures. The molecular and crystal structure diagrams drawings were generated using PLATON [37]. Database searches were undertaken using the Cambridge Structural Database [31].

4.2. General procedure for the synthesis of N-para-ferrocenyl benzoyl amino acid esters *1–8*

4.2.1. N-{para-(ferrocenyl)benzoyl} glycine ethyl ester *1*

Glycine ethyl ester hydrochloride (0.3 g, 2.2 mmol) and triethylamine (0.5 ml) were added to a solution of *para*-ferrocenyl benzoic acid (0.5 g, 1.6 mmol), 1-hydroxybenzotriazole (0.3 g, 2.2 mmol) and 1,3-dicyclohexylcarbodiimide (0.45 g, 2.2 mmol) in CH_2Cl_2 (50 ml) at 0 °C. After 30 min, the solution was raised to room temperature and allowed to proceed for 48 h. The precipitated *N,N*-dicyclohexylurea was removed by filtration and the filtrate washed with water, 10% potassium hydrogen carbonate, 5% citric acid and dried over $MgSO_4$. Recrystallization from petroleum ether (40–60 °C): ethyl acetate furnished the title compound as orange needles. The crystals were of sufficient quality for an X-ray diffraction study (0.351 g, 56%).

m.p. 102–104 °C, $E_{1/2}$ = 513 mV.
Mass spectrum: found: $[M]^{+\cdot}$ 391,
$C_{21}H_{21}N_1O_3Fe$ requires: 391.
I.R. ν_{max} (KBr): 3308, 1735, 1700, 1685, 1211 cm^{-1}.
UV–Vis λ_{max} CH_2Cl_2: 358 (ε 2290), 454 (ε 740) nm.

^{1}H NMR (400 MHz) δ (DMSO): 8.90 (1H, d, J = 7.6 Hz –CON*H*–), 7.79 (2H, d, J = 8 Hz, ArH), 7.64 (2H, d, J = 8 Hz, ArH), 4.89 {2H, t, J = 2 Hz, *ortho* on (η^5-C_5H_4)}, 4.41 {2H, t, J = 2 Hz, *meta* on (η^5-C_5H_4)}, 4.12 (2H, q, J = 7.2 Hz, –OC*H*$_2$CH$_3$), 4.02 {5H, s, (η^5-C_5H_5)}, 3.99 (2H, d, J = 5.6 Hz, –NHC*H*$_2$CO–), 1.21 (3H, t, J = 7.2 Hz, –OCH$_2$C*H*$_3$).

^{13}C NMR (100 MHz) δ (DMSO): 170.4, 166.9, 143.4, 131.0, 127.8, 125.8, 83.5, 69.9, 67.0, 60.8 (−ve DEPT), 33.7 (−ve DEPT), 14.4.

4.2.2. N-{para-(ferrocenyl)benzoyl}-L-alanine ethyl ester **2**

L-Alanine ethyl ester hydrochloride (0.3 g, 2.0 mmol) was used. Recrystallization from petroleum ether (40–60 °C): ethyl acetate furnished the title compound as an orange solid (0.38 g, 59%).

m.p. 104–106 °C, $E_{1/2}$ = 505 mV,
$[\alpha]_D^{25} = +28^\circ$ (c = 2.1, EtOH).
Mass spectrum: found: $[M]^{+\cdot}$ 405,
$C_{22}H_{23}N_1O_3Fe$ requires: 405.
I.R. ν_{max} (KBr): 2928, 1750, 1648, 1509 cm^{-1}.
UV–Vis λ_{max} CH_2Cl_2: 358 (ε 2670), 454 (ε 860) nm.

^{1}H NMR (400 MHz) δ (DMSO): 8.47 (1H, d, J = 6.8 Hz, –CON*H*–), 7.56 (2H, d, J = 8 Hz, ArH), 7.38 (2H, d, J = 8 Hz, ArH), 4.65 {2H, s, *ortho* on (η^5-C_5H_4)}, 4.41–4.48 {1H, m, –C*H*(CH$_3$)}, 4.17 {2H, s, *meta* on (η^5-C_5H_4)}, 4.12 (2H, q, J = 7.6 Hz, –OC*H*$_2$CH$_3$), 3.77 {5H, s, (η^5-C_5H_5)}, 1.48 {3H, d, J = 7.2 Hz, –CH(C*H*$_3$)}, 1.21 (3H, t, J = 7.6 Hz, –OCH$_2$C*H*$_3$).

^{13}C NMR (100 MHz) δ (DMSO): 173.5, 166.5, 143.3, 131.1, 128.0, 125.7, 83.5, 69.9, 67.0, 60.8 (−ve DEPT), 48.7, 17.1, 14.5.

4.2.3. N-{para-(ferrocenyl)benzoyl}-L-leucine ethyl ester **3**

L-Leucine ethyl ester hydrochloride (0.3 g, 1.5 mmol) was used. Recrystallization from petroleum ether (40–60 °C): ethyl acetate furnished the title compound as brown solid (0.46 g, 68%).

m.p. 127–129 °C, $E_{1/2}$ = 501 mV,
$[\alpha]_D^{20} = +3^\circ$ (c = 1.2, EtOH).
Mass spectrum: found: $[M]^{+\cdot}$ 447,
$C_{25}H_{29}N_1O_3Fe$ requires: 447.
I.R. ν_{max} (KBr): 3331, 2933, 1728, 1614 cm^{-1}.
UV–Vis λ_{max} CH_2Cl_2: 352 (ε 1550), 454 (ε 450) nm.

^{1}H NMR (400 MHz) δ (DMSO): 8.66 (1H, d, J = 7.6 Hz, –CON*H*–), 7.80 (2H, d, J = 8 Hz, –ArH), 7.62 (2H, d, J = 8 Hz, –ArH), 4.88 {2H, s, *ortho* on (η^5-C_5H_4)}, 4.50–4.60 [1H, m, –C*H*{CH$_2$CH(CH$_3$)$_2$}], 4.41 {2H, s, *meta* on (η^5-C_5H_4)}, 4.08 (2H, q, J = 6.8 Hz, –OC*H*$_2$CH$_3$), 4.02 {5H, s, (η^5-C_5H_5)}, 1.57–1.81 [3H, m, –CH{C*H*$_2$C*H*(CH$_3$)$_2$}], 1.19 (3H, t, J = 6.8 Hz, –OCH$_2$C*H*$_3$), 0.93 [3H, d, J = 6.4 Hz, –CH{CH$_2$CH(C*H*$_3$)$_2$}], 0.86 [3H, d, J = 6.4 Hz, –CH{CH$_2$CH(C*H*$_3$)$_2$}].

^{13}C NMR (100 MHz) δ (DMSO): 173.1, 166.9, 143.3, 131.1, 128.0, 125.7, 83.5, 69.9, 67.0, 60.1 (−ve DEPT), 51.4, 39.6 (−ve DEPT), 24.8, 23.2, 21.5, 14.4.

4.2.4. N-{para-(ferrocenyl)benzoyl}-L-phenylalanine ethyl ester **4**

L-Phenylalanine ethyl ester hydrochloride (0.3 g, 1.3 mmol) was used. Recrystallization from petroleum ether (40–60 °C): ethyl acetate furnished the title compound as an orange solid (0.38 g, 61%).

m.p. 134–136 °C, $E_{1/2}$ = 498 mV,
$[\alpha]_D^{20} = +48^\circ$ (c = 2, EtOH).
Mass spectrum: found: $[M]^{+\cdot}$ 481,
$C_{28}H_{27}N_1O_3Fe$ requires: 481.
I.R. ν_{max} (KBr): 2929, 1710, 1636, 1106 cm^{-1}.
UV–Vis λ_{max} CH_2Cl_2: 358 (ε 3370), 454 (ε 1070) nm.

^{1}H NMR (400 MHz) δ (DMSO): 8.80 (1H, d, J = 7.6 Hz, –CON*H*–), 7.73 (2H, d, J = 8.4 Hz, –ArH), 7.61 (2H, d, J = 8.4 Hz, –ArH), 7.21–7.32 (5H, m, –ArH), 4.88 {2H, s, *ortho* on (η^5-C_5H_4)}, 4.54–4.68 {1H, m, –C*H* (CH$_2$Ph)}, 4.41 {2H, s, *meta* on (η^5-C_5H_4)}, 4.10 (2H, q, J = 7.2 Hz, –OC*H*$_2$CH$_3$), 4.02 {5H, s, (η^5-C_5H_5)}, 3.11–3.17 {2H, m, –CH(C*H*$_2$Ph)}, 1.16 (3H, t, J = 7.2 Hz, –OCH$_2$C*H*$_3$).

^{13}C NMR (100 MHz) δ (DMSO): 172.3, 166.8, 143.4, 138.0, 131.1, 129.4, 128.6, 127.9, 126.9, 125.7, 83.5, 69.9, 68.1, 67.1, 66.9, 61.0 (−ve DEPT), 54.8, 33.7 (−ve DEPT), 14.4.

4.2.5. N-{para-(ferrocenyl)benzoyl}-β-alanine ethyl ester **5**

β-Alanine ethyl ester hydrochloride (0.3 g, 2.0 mmol) was used. Recrystallization from diethyl ether furnished the title compound as orange needles (0.34 g, 52%).

m.p. 137–138 °C, E'° = 131 mV.
Mass spectrum: found: $[M + H]^+$ 406.1080,
$C_{22}H_{24}N_1O_3Fe$ requires: 406.1106.
I.R. ν_{max} (KBr): 2930, 1708, 1651, 1629 cm^{-1}.
UV–Vis λ_{max} CH_2Cl_2: 354 (ε 1900), 452 (590) nm.

^{1}H NMR (400 MHz) δ (DMSO): 8.56 (1H, t, J = 5.2 Hz, –CON*H*–), 7.76 (2H, d, J = 8 Hz, –ArH), 7.61 (2H, d, J = 8 Hz, –ArH), 4.87 {2H}, s, *ortho* on (η^5-C_5H_4)}, 4.39 {2H, s, *meta* on (η^5-C_5H_4)}, 4.07 (2H, q, J = 7.6 Hz, –OC*H*$_2$CH$_3$), 4.01 {5H, s, (η^5-C_5H_5)}, 3.50 (2H, q, J = 7.2 Hz, –C*H*$_2$CH$_2$–), 2.59

(2H, t, $J = 7.2$ Hz, –CH_2CH_2–), 1.18 (3H, t, $J = 7.6$ Hz, –OCH_2CH_3).

^{13}C NMR (100 MHz) δ(DMSO): 171.7, 166.5, 143.0, 131.7, 127.7, 125.7, 83.6, 69.8, 66.9, 60.3 (−ve DEPT), 34.2 (−ve DEPT), 31.0 (−ve DEPT), 14.0.

4.2.6. N-{para-(ferrocenyl)benzoyl}-4-aminobutyric acid ethyl ester **6**

4-Aminobutyric acid ethyl ester hydrochloride (0.3 g, 1.8 mmol) was used. Recrystallization from diethyl ether furnished the title compound as orange needles (0.37 g, 55%).

m.p. 80–82 °C, $E'^{\circ} = 132$ mV.
Mass spectrum found: $[M + H]^+$ 420.1264,
$C_{23}H_{26}N_1O_3Fe$ requires: 420.1262,
I.R. ν_{max} (KBr): 2930, 1733, 1623, 1547 cm^{-1}.
UV–Vis λ_{max} CH_2Cl_2: 354 (ε 1260), 450 (ε 370) nm.

^{1}H NMR (400 MHz) δ (DMSO): 8.45 (1H, t, $J = 5.2$ Hz, –CON*H*–), 7.77 (2H, d, $J = 8$ Hz, –ArH), 7.61 (2H, d, $J = 8$ Hz, –ArH), 4.88 {2H, s, *ortho* on (η^5-C_5H_4)}, 4.40 {2H, s, *meta* on (η^5-C_5H_4)}, 4.06 (2H, q, $J = 7.6$ Hz, –OCH_2CH_3), 4.02 {5H, s, (η^5-C_5H_5)}, 3.39 (2H, q, $J = 7.2$ Hz, –$NHCH_2CH_2CH_2$–), 2.36 (2H, t, $J = 7.2$ Hz, –$NHCH_2CH_2CH_2$–), 1.78 (2H, quint, $J = 7.2$ Hz, –$NHCH_2CH_2CH_2$–), 1.17 (3H, t, $J = 7.6$ Hz, –OCH_2CH_3).

^{13}C NMR (100 MHz) δ (DMSO): 173.1, 166.4, 142.8, 131.9, 127.7, 125.7, 83.6, 69.8, 66.9, 60.1 (−ve DEPT), 33.7 (−ve DEPT), 31.4 (−ve DEPT), 24.9 (−ve DEPT), 14.5.

4.2.7. N-{para-(ferrocenyl) benzoyl} (±)-2-aminobutyric acid ethyl ester **7**

(±)-2-Aminobutyric acid ethyl ester hydrochloride (0.3 g, 1.8 mmol) was used. Recrystallization from petroleum ether (40–60°) furnished the title compound as orange needles. The crystals were of sufficient quality for an X-ray diffraction study (0.37 g, 55%).

m.p. 105–107 °C, $E'^{\circ} = 136$ mV.
Mass spectrum: found: $[M]^{+\cdot}$ 419.105,
$C_{23}H_{25}N_1O_3Fe$ requires: 419.118.
I.R. ν_{max} (KBr): 3305, 2981, 2928, 1734, 1639, 1609, 1542, 1522 cm^{-1}.
UV–Vis λ_{max} MeCN: 350 (ε 1190), 451 (ε 350) nm.

^{1}H NMR (400 MHz) δ ($CDCl_3$): 7.66 (2H, d, $J = 8.4$ Hz, ArH), 7.44 (2H, d, $J = 8.4$ Hz, ArH), 6.69 (1H, d, $J = 7.6$ Hz, –CON*H*–), 4.72 {1H, q, $J = 6.4$ Hz, –C*H*(CH_2CH_3)}, 4.63 {2H, s, *ortho* on (η^5-C_5H_4)}, 4.31 {2H, s, *meta* on (η^5-C_5H_4)}, 4.18 (2H, q, $J = 7.2$ Hz, –OCH_2CH_3), 3.96 {5H, s, (η^5-C_5H_5)}, 1.91–1.98 {1H, m, –CH(C*H*$_2$$CH_3$)}, 1.74–1.89 {1H, m, –CH(C*H*$_2$$CH_3$)}, 1.24 (3H, t, $J = 7.2$ Hz, –OCH_2CH_3), 0.91 {3H, t, $J = 7.2$ Hz, CH(CH_2CH_3)}.

^{13}C NMR (100 MHz) δ ($CDCl_3$): 173.1, 167.3, 144.2, 131.5, 127.6, 126.2, 83.9, 70.2, 70.1, 67.2, 61.9 (−ve DEPT), 54.0, 26.2 (−ve DEPT), 14.6, 9.9.

4.2.8. N-{para-(ferrocenyl) benzoyl}-isobutyricacid ethyl ester **8**

Isobutyric acid ethyl ester hydrochloride (0.3 g, 1.8 mmol) was used. Recrystallization from diethyl ether furnished the title compound as an orange solid (0.22 g, 55%).

m.p. 130–132 °C, $E'^{\circ} = 132$ mV.
Mass spectrum: found: $[M]^{+\cdot}$ 419.110,
$C_{23}H_{25}N_1O_3Fe$ requires: 419.118.
I.R. ν_{max} (KBr): 3223, 2928, 1741, 1621, 1610, 1567, 1521 cm^{-1}.
UV–Vis λ_{max} MeCN: 367 (ε 2900), 453 (ε 1060) nm.

1H NMR (400 MHz) δ ($CDCl_3$): 7.64 (2H, d, $J = 8$ Hz, ArH), 7.44 (2H, d, $J = 8$ Hz, ArH), 6.77 (1H, s, –CON*H*–), 4.63 {2H, s, *ortho* on (η^5-C_5H_4)}, 4.31 {2H, s, *meta* on (η^5-C_5H_4)}, 4.19 (2H, q, $J = 7.2$ Hz, –OCH_2CH_3), 3.97 {5H, s, (η^5-C_5H_5)}, 1.63 {6H, s, –C(CH_3)$_2$}, 1.23 (3H, t, $J = 7.2$ Hz, –OCH_2CH_3).

^{13}C NMR (100 MHz) δ ($CDCl_3$): 175.4, 166.8, 143.9, 132.2, 127.5, 126.2, 83.9, 70.2, 70.0, 67.1, 62.1 (−ve DEPT), 57.3, 25.1, 14.6.

4.3. Crystallographic footnotes for (**1**) and (**7**)

Crystallographic data **1**: chemical formula $C_{21}H_{21}NO_3Fe$, red block, molecular weight 391.24 g mol^{-1}, monoclinic, space group $P2_1/c$ (No. 14), $a = 15.417(2)$, $b = 9.712(3)$, $c = 25.084(4)$ Å, $\beta = 97.740(5)°$, $V = 3721.4(13)$ Å^3, $Z = 8$, density = 1.397 g cm^{-3} (calc.), $F(0\,0\,0) = 1632$, $\mu = 0.830$ mm^{-1}, absorption correction range 0.746–0.960, 9666 reflections in the range 2–26°, 7332 unique, $3336 > 2\sigma(I)$, 259 parameters, R factor = 0.070, $wR_2 = 0.136$, GOF = 1.02, density range in the final difference map is −0.38 to +0.35 e Å^{-3} (highest peaks in close proximity to the ester ethoxy group and iron atom).

Crystallographic data **7**: chemical formula $C_{23}H_{25}NO_3Fe$, red block, molecular weight 419.29 g mol^{-1}, monoclinic, space group $P2_1/c$ (No. 14), $a = 14.500(2)$, $b = 9.4360(10)$, $c = 15.316(2)$ Å, $\beta = 105.940(10)°$, $V = 2015.0(4)$ Å^3, $Z = 4$, density = 1.382 g.cm^{-3} (calc.), $F(0\,0\,0) = 880$, $\mu = 0.772$ mm^{-1}, absorption correction range 0.699–0.723, 10122 reflections in the range 2–28°, 4890 unique, $3785 > 2\sigma(I)$, 259 parameters, R factor = 0.047, $wR_2 = 0.118$, GOF = 1.03, density range in the final difference map is −0.63 to +0.58 e Å^{-3} (highest peaks in close proximity to the iron atom).

5. Supplementary material

Crystallographic data for the structural analyses have been deposited with the Cambridge Crystallographic Data Centre, CCDC numbers **235738** and **235739** for **1** and **7**, respectively. Copies of this information may be obtained free of charge from The Director, CCDC, 12 Union road, Cambridge, CB2 1EZ, UK (fax: +44-1223-336033; e-mail: deposit@ccdc.cam.ac.uk).

Acknowledgements

DS thanks the Irish American Partnership and Dublin City University for the funding of a studentship award 1999–2002. We also thank Ms Kimiko Shiohara for FABMS measurements.

References

[1] (a) G. Jaouen (Ed.), J. Organomet. Chem., 589, 1999, pp. 1–126; (b) R.D. Adams (Ed.), J. Organomet. Chem., 619, 1999, pp. 1–875.
[2] V. Degani, A. Heller, J. Am. Chem. Soc. 110 (1988) 2615.
[3] M. Kira, T. Matsubara, H. Shinohara, M. Sisido, Chem. Lett. (1997) 89.
[4] H.-B. Kraatz, J. Lusztyk, G.D. Enright, Inorg. Chem. 36 (1997) 2400.
[5] J.F. Gallagher, P.T.M. Kenny, M.J. Sheehy, Inorg. Chem. Commun. 2 (1999) 327.
[6] A. Nomoto, T. Moriuchi, S. Yamazaki, A. Ogawa, T. Hirao, J. Chem. Soc. Chem. Commun. (1998) 1963.
[7] T. Moriuchi, A. Nomoto, K. Yoshida, A. Ogawa, T. Hirao, J. Am. Chem. Soc. 123 (2001) 68.
[8] T. Moriuchi, A. Nomoto, K. Yoshida, T. Hirao, Organometallics 20 (2001) 1008.
[9] T. Itoh, S. Shirakami, N. Ishida, Y. Yamashita, T. Yoshida, H.-S. Kim, Y. Wataya, Bioorg. Med. Chem. Lett. 10 (2000) 1657.
[10] J.F. Gallagher, P.T.M. Kenny, M.J. Sheehy, Inorg. Chem. Commun. 2 (1999) 200.
[11] H.-B. Kraatz, D.M. Leek, A. Houmam, G.D. Enright, J. Lusztyk, D.D.M. Wayner, J. Organomet. Chem. 589 (1999) 38.
[12] A. Hess, J. Sehnert, T. Weyhermüller, N. Metzler-Nolte, Inorg. Chem. 39 (2000) 5437.
[13] O. Brosch, T. Weyhermüller, N. Metzler-Nolte, Inorg. Chem. 39 (2000) 323.
[14] T. Moriuchi, K. Yoshida, T. Hirao, Organometallics 20 (2001) 3101.
[15] Y.M. Xu, H.-B. Kraatz, Tet. Lett. 42 (2001) 2601.
[16] T. Moriuchi, K. Yoshida, T. Hirao, J. Organomet. Chem. 637 (2001) 75.
[17] A. Wieckowska, R. Bilewicz, A. Misicka, M. Pietraszkiewicz, K. Bajdor, L. Piela, Chem. Phys. Lett. 350 (2001) 447.
[18] H.-B. Kraatz, Y.M. Xu, P. Saweczko, J. Organomet. Chem. 637 (2001) 335.
[19] P. Stepnicka, I. Cisarova, New J. Chem. 26 (2002) 1389.
[20] S. Maricic, U. Berg, T. Frejd, Tetrahedron 58 (2002) 3085.
[21] S. Maricic, T. Frejd, J. Org. Chem. 67 (2002) 7600.
[22] D. Savage, J.F. Gallagher, Y. Ida, P.T.M. Kenny, Inorg. Chem. Commun. 5 (2002) 1034.
[23] D.R. van Staveren, T. Weyhermuller, N. Metzler-Nolte, J. Chem. Soc. Dalton Trans. (2003) 210.
[24] J.L. Kuo, J.H. Liao, C.T. Chen, C.H. Huang, C.S. Chen, J.M. Fang, Org. Lett. 5 (2003) 1821.
[25] M.J. Sheehy, J.F. Gallagher, M. Yamashita, Y. Ida, J. White-Colangelo, J. Johnson, R. Orlando, P.T.M. Kenny, J. Organomet. Chem. 689 (2004) 1511.
[26] M. Barber, R.S. Bordoli, R.D. Sedgwick, A.N. Tyler, J. Chem. Soc. Chem. Commun. (1981) 325.
[27] J.B. Fenn, J. Am. Soc. Mass Spectrom. 4 (1993) 524.
[28] M. Karas, D. Bachmann, U. Bahr, F. Hillenkamp, Int. J. Mass Spectrom. Ion Processes 78 (1987) 53.
[29] K. Tanaka, H. Waki, Y. Ido, S. Akita, Y. Yoshida, T. Yoshida, Rapid Commun. Mass Spectrom. 2 (1988) 151.
[30] T. Donovan McCarley, R.L. McCarley, P.A. Limbach, Anal. Chem. 70 (1998) 4376.
[31] F.H. Allen, O. Kennard, Chem. Des. Automat. News 8 (1993) 131.
[32] A. Bavaso, E. Benedetti, B. Diblasio, G. Morelli, C. Pedone, Acta Crystallogr. B 37 (1981) 1132.
[33] B. Kojic-Prodic, B. Nigovic, D. Horvatic, Z. Ruzic-Toros, V. Magnus, W.L. Duax, J.J. Stezowski, N. Bresciani-Pahor, Acta Crystallogr. B 47 (1991) 107.
[34] C.H. Gorbitz, Acta Crystallogr. C 58 (2002) o533.
[35] J. Voogd, J.L. Derissen, Acta Crystallogr. B 36 (1980) 3175.
[36] G.M. Sheldrick, SHELXL97, University of Göttingen, Göttingen, 1997.
[37] A.L. Spek, PLATON, University of Utrecht, Holland, 1998.